



Metrology of angles in astronomy

Jean Kovalevsky¹

Observatoire de la Côte d'Azur, avenue Copernic, 06130 Grasse, France

Presented by Guy Laval

Abstract

In astronomy, measurements of angles play a major role. After defining the units in use in astronomy, three methods of measuring angles are presented, with an application to the transit instrument. The interferometric techniques for measuring large angles are described in optical and radio wavelengths. Due to the atmospheric and mechanical limitation on ground, space astrometry has multiple advantages. The satellite Hipparcos is described and the data reduction procedures and results obtained are sketched. In the future, two new astrometric space missions are approved: GAIA, based on Hipparcos principles and SIM, a space interferometer. They are described and the expected accuracies are presented. *To cite this article: J. Kovalevsky, C. R. Physique 5 (2004).*

© 2004 Académie des sciences. Published by Elsevier SAS. All rights reserved.

Résumé

Métrie des angles en astronomie. En astronomie, les mesures angulaires jouent un grand rôle. Après avoir défini les unités en usage en astronomie, trois méthodes de mesure sont présentées, appliquées à l'instrument méridien. On décrit les techniques interférométriques pour mesurer les grands angles dans les domaines optiques et radio. Par suite des limitations d'origine atmosphérique ou mécanique de l'astronomie au sol, l'astrométrie spatiale présente de nombreux avantages. On donne un aperçu du satellite Hipparcos ainsi que des méthodes de réduction des données et des résultats obtenus. Dans l'avenir, deux nouvelles missions spatiales astrométriques sont approuvées : GAIA, basé sur le principe d'Hipparcos et SIM, un interféromètre spatial. Elles sont décrites et l'on présente les exactitudes attendues. *Pour citer cet article : J. Kovalevsky, C. R. Physique 5 (2004).*

© 2004 Académie des sciences. Published by Elsevier SAS. All rights reserved.

Keywords: Angles; Astronomy; Space; Interferometry

Mots-clés : Angles ; Astrométrie ; Espace ; Interférométrie

1. Units of angle

Angles are a geometric dimensionless measurable quantities. In the SI, the unit is the radian (symbol rad). It is the most natural unit because of the properties of the derivatives in trigonometric functions so fundamental in kinematics and all periodic

E-mail address: jean.kovalevsky@obs-azur.fr (J. Kovalevsky).

¹ Emeritus President of the CIPM.

phenomena. In contrast, it is a very awkward unit for the measurement of angles, except very small ones. This is because the natural method in measuring angles is to compare them with a regularly divided circle, an artefact that is impossible to build when the divisions are incommensurable with a complete rotation.

So, in practice, in laboratories, one uses as the fundamental unit the circumference, which is the rotation angle that bring back to the original direction, and a rational subdivision of it, namely the degree (symbol $^\circ$), the 360th part of a circumference. For smaller angles, one uses

- the minute (of a degree) or minute, symbol $' = 1^\circ/60$ and
- the second (of a degree) or second, symbol $'' = 1^\circ/3600$.

In astronomy, an old science where traditions are vivid, the degree, minute and second are still almost universally used, even if there is now a trend to introduce the decimal degree, as recommended by ISO. But because, in many instances, time and angles are present simultaneously in measuring procedures, the angular minutes and seconds are generally called 'arcminutes' and 'arcseconds'.

Another long-lived tradition is to be noted; the angles on the sky along the equator were measured by the time difference between their transits through a local meridian. The time scale ruling the rotation of the Earth with respect to stars is the sidereal time (24 hours of sidereal time are 24 hours of Universal time minus 236.5554 s). Astronomers took the habit of using sidereal time differences to express angles as right ascensions or hour angles in hours ($= 15^\circ$), minutes ($= 15'$) or seconds ($= 15''$). Although it is still used in many star catalogues, this is a disturbing habit, because these units are not applicable to measurements in other directions.

Another characteristic of modern astronomy is that it deals with smaller and smaller angles. Since, in the past, arcseconds were used (for instance to express stellar parallaxes), the natural trend was to introduce decimal subdivisions of the arcsecond. At present, there are two subunits that we shall use in this paper:

- the milliarcsecond (symbol mas) $= 0.001'' = 4.848\ 14 \times 10^{-9}$ rad and
- the microarcsecond (symbol μ as) $= 0.001$ mas $= 4.848 \times 10^{-12}$ rad.

It would be better to use nano- and picoradians, but this would mean inconsistencies in the units used for small and large angles.

2. Measuring angles

The natural standard of angles is the circumference, but it is not materialised as such. In practice, there are three ways of realising angles in a large range of values. These are:

2.1. The divided circle

It is a wheel, centred on the axis of rotation from which directions are to be determined. On its edge, engraved marks are equally distant graduations over the circumference. They are engraved by a dividing machine, which rotates in predetermined sequences. A current interval is 3 arcminutes. The measuring device includes microscopes and a vernier scale that allows interpolations.

Whatever is care with which the engraving, the circularity, and the centring of the wheel are achieved, there remains large and small scale errors, and a calibration must be performed and, periodically redone. The method uses two pairs of microscopes aligned with the assumed rotation axis of the wheel separated by a reference angle, which is approximately a rational fraction of the circumference. The wheel is turned in such a way that to the marks seen by the first pair of microscopes correspond to marks seen by the second and offsets are measured. This is performed as many times as necessary for the circle to return to the original position. Then the standard angle is changed, and the procedure is repeated until all the graduations have been measured, and there are enough equations linking the offsets. A detailed description is given in [1]. The accuracy of the best divided circles is of the order of $0.03''$.

2.2. Measuring angles by a rotation

The principle is to use the rotation of a rigid body. If the law of rotation is sufficiently well modelled, the measurement reduces to the determination of the time interval that separates the orientations at times t_1 and t_2 . In astronomy, the rotation of the Earth is now determined with an accuracy of 0.1 mas. The rotation speed of the Earth is such that this angle is crossed in

0.07 ms, a very easy precision to achieve with modern clocks. We shall give later in this article an example of how this method is applied in space astronomy.

2.3. Measurement of small angles

In astronomy, a current objective is to determine the relative angular position of stars in a small field of view, typically a few square degrees. This was done producing the image of a portion of the sky through a telescope and recorded formerly on a photographic plate (up to $6^\circ \times 6^\circ$) which was digitised by a measuring machine, giving the position X of the image in some coordinate system in the plate. Now, the image is formed on CCD arrays. The latter have the advantages to be much more sensitive and to provide directly an electronic digitised image, but even the largest set of CCDs displayed on the focal plane does not cover such a large field of view.

There is a complex transformation between the relative spherical coordinates of stars ($\Delta\alpha$, $\Delta\delta$) with respect to some central point of the field, and the rectangular coordinates measured on the plane of the receiver. It takes into account:

- The gnomonic, or conical, transformation from a sphere to a tangent plane;
- The atmospheric refraction as a function of the zenith distance of the star and its colour;
- All optical aberrations of the telescope (defocus, spherical aberration, distortion, astigmatism, coma);
- The non-rigorous dispositions of the CCDs on a plane;
- A shift of the centroid of the image, which depends on the luminosity and the colour of the star.

The ensemble of these effects is modelled by a polynomial development giving the measured plane coordinates of the image, X , as a function of the correction $\Delta\alpha$, $\Delta\delta$ to the relative spherical coordinates and corrections to all the relevant parameters P_i among those mentioned above.

$$X = F(\Delta\alpha, \Delta\delta, \Delta P_1, \dots, \Delta P_n). \quad (1)$$

The method is relative. It is necessary to know a priori the positions of N stars and the corresponding positions, X , of their images, to solve first the $2N$ equations (1) for the unknown parameters. An iterative procedure is generally necessary to converge to a stable solution.

With long foci instruments, internal uncertainties of the order of a few hundredths of an arc second can be achieved. Detailed description of these methods can be found in [2].

3. The transit instrument

The transit instrument (or meridian circle) has been, for almost two centuries, the basic instrument for astrometry. It is now superseded by space astrometry, but it is worthwhile mentioning it, not only to illustrate the progress which has been made, but also because it encompasses the two main methods to measure large angles.

It consists essentially of a tube holding the objective of a refractor and rotating around a horizontal East–West axis, materialised by the axis of two cylindrical pivots supported by V-shape bearings fastened on piers, strongly anchored in rock to ensure stability. The direction of the observation is specified by the optical axis of a refractor, whose aperture and focal length are generally of the order of 20 cm and 3 metres respectively. They are insulated and are independent of the floor.

The declination or the altitude of an object is measured using a divided vertical circle centred on the East–West axis and rigidly fixed to it, so that it rotates with the tube and consequently with the optical axis. The divisions of the circle are read simultaneously by several microscopes or cameras.

At the focus of the objective there is a micrometer associated with a clock. It is used to determine the time at which the star image crosses the vertical plane defined by the optical axis of the instrument. In an ideal perfect instrument, it is the local meridian. Knowing the orientation of the Earth as a function of time from Earth rotation independent observations, one derives the right ascension of the object.

However, of course, the actual instrument does not realise exactly the ideal theoretical structure. Although the construction is as rigid as possible and the orientation of the instrument is set with maximum care, fixed and variable orientation defects are inevitable. They have to be determined and introduced in the reduction procedure (see [3]).

4. Interferometric techniques

A major advance in astrometry from the ground came when interferometric techniques started to be used for astrometry. Let us present the principle of Michelson (or phase) interferometry as applied to the determination of positions of stars.

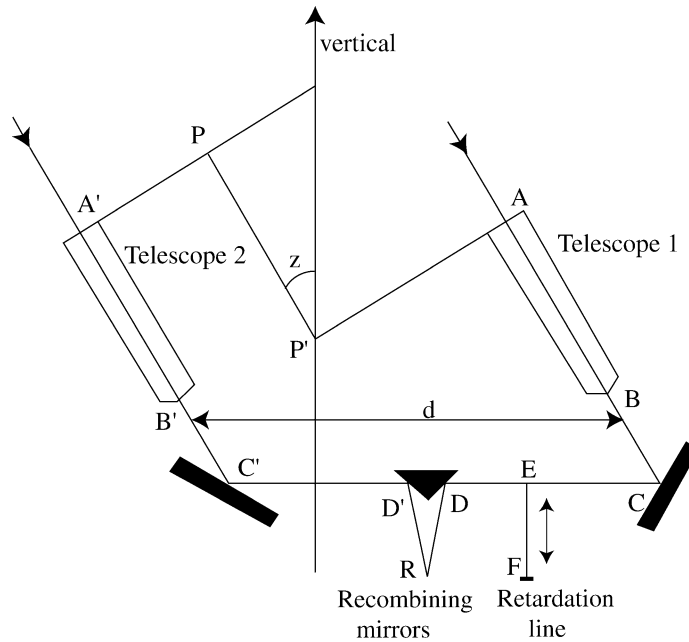


Fig. 1. Principle of a Michelson (or phase) interferometer.

4.1. Optical stellar interferometry

Let two identical telescopes point at some given star. Let us assume first that it is a point-like source so that all rays in a plane perpendicular to the direction of a star have the same phase. Mirrors are placed in such a way that the two beams are recombined into a single one. Interference fringes appear when the difference of light paths is smaller than the coherence length of the incoming beams, and the central fringe corresponds to a strict equality of optical paths. Fig. 1 presents a schematic view of such an interferometer, assuming for clarity that the star and the two axes of the telescopes are in the same vertical plane. If R is the receiver, let us write that the optical paths from the wavefront P is equal for both telescopes:

$$A'B' + B'C' + C'D' + D'R = PP' + AB + BC + CE + 2EF + ED + DR. \tag{2}$$

The position of the ensemble DD' and R is fixed. In order to achieve this equality while the Earth rotates and therefore the various lengths vary, an additional path length on CD is provided by a delay line EF, which is set in such a way that the light is directed at E towards F. In F a mirror reflects it back to E and the light is then sent towards D and the receiver. The mirror F is servo-controlled by R in such a way that R always receives the central fringe, so that Eq. (2) is always satisfied. When the central fringe appears on R, it is surrounded by the interferometric pattern built up by the two beams. The path difference, $PP' = \Delta x$ is obtained by measuring the additional path $2EF$ in the delay line, the other quantities in (2) are calibrated by laser interferometry.

If z is the zenith distance of the star and d is the distance between the axes of the two telescopes, the path difference is $\Delta x = d \sin z$. This can be extended to any configuration of the interferometer. Let, in some local system of coordinates, the unit vector of the direction of the star be \mathbf{S} , and \mathbf{B} be the base vector of the interferometer, one has

$$\Delta x = \mathbf{S} \times \mathbf{B}. \tag{3}$$

In other terms, measuring Δx gives a relation between the apparent direction of the star and the base vector attached to the Earth. Observing several stars at different times of the night, so that the geometry with respect to the baseline varies, one obtains the relative positions of the stars on the celestial sphere.

The main limitations in Michelson astrometric interferometry are:

- the stability of the baseline throughout the night;
- the accuracy of the laser interferometers, which monitor the positions of the optical design;
- the evaluation of the refraction in a consistent manner throughout the night;
- the instability and the deformation of the wave front due to atmospheric turbulence giving rise to a stochastic additional error in the optical path difference.

The ensemble of these limitations prevent stellar interferometers reaching the theoretical resolving power $s \sim \lambda/d$, where λ is the wavelength.

4.2. Imaging mode

The measurement of large angles by interferometry is very difficult because it is based on the analysis of phases. It was tested in the early 1990s at the Mount Wilson Observatory. A description of the instruments can be found in [4] and a general review of the field is given in [5]. Several of the difficulties of the phase interferometry mentioned above are avoided if one measures only the intensity of the central fringe.

We have assumed in the preceding section, that the sources are point-like sources. The objective of amplitude interferometry is to obtain information on the light distribution of an extended source. Such a source consists in a number of incoherent point-like sources, each of them producing independent system of fringes. What is observed is the sum (or the integral) of the illuminations produced by each point of the source. If the source is small, the fringes are still observable, but are blurred. In particular, the intensity of the central fringe is reduced to I_{\max} and the minimum of intensity is not zero, but I_{\min} . One defines the fringe visibility by:

$$V = (I_{\max} - I_{\min}) / (I_{\max} + I_{\min}). \quad (4)$$

The most frequent application is the measurement of apparent stellar diameters D . The principle of such measurements is described in [6]. If one assumes that the apparent brightness of the star is constant over its surface, the visibility is given by

$$V = [2J_1(BD\pi/\lambda)] / (BD\pi/\lambda), \quad (5)$$

where J_1 is the Bessel function, B is the projected baseline, and λ the wavelength. Different visibilities are measured by observing at different times and/or by moving the telescopes so that B takes different values. Then, D is obtained by solving Eqs. (5). Of course, there is a need of calibrating the instrument so that instrumental parameters are added to Eqs. (5). One can also vary the wavelengths. More refined analyses of a set of observations allows one also to image the star [7] and to determine the centre to limb darkening of a star [8].

Another application is the measurement of the separation and the magnitudes of double stars. In addition to B and λ , the theoretical visibility curves are modelled as functions of the angular separation vector between the components, the intensity ratio, and the intrinsic visibility of each component as given by Eq. (4); see [9]. Again, using a large number of observation equations obtained under different conditions, one derives the unknown parameters. If the time span is sufficiently long so that the relative positions of the components have varied, one may in addition determine some characteristics of the orbit; see for instance, [10].

At present, the most powerful instrument for intensity interferometry is the CHARA (Center for High Angular Resolution Astronomy) array. It is a six interconnected 1 metre individual telescopes array located at the Mount Wilson Observatory grounds. The largest baseline is 330 m. The light from the telescopes is conveyed to the central beam synthesis facility through vacuum tubes. The length of the baselines is known with accuracies better than one micrometre. It is now in operation, with an ultimate goal of achieving 0.2 mas accuracy in the measurement of star diameters and the separation of double star components. This objective is not yet reached, but improvements are continuously carried out in cooperation with groups offering technologies for enhanced performance. At present, the cooperation is essentially with French groups: Paris Observatory, which has provided its 'Fiber Linked Unit for Optical Recombination' and the Astrophysical Observatory of Grenoble with which a highly compact multi-beam combiner using the technology of integrated optics is being developed.

4.3. The Navy Prototype Optical Interferometer

Although several stellar interferometers are in service in the world, they are used for imaging purposes as described above. The only exception is the Navy Prototype Optical Interferometer (NPOI) in Lowell Observatory (Arizona). It consists in three 250 m legs in a Y configuration with stations for imaging siderostats providing baselines between 2 m and 440 m. It contains also a phase interferometry facility designed for astrometry. It consists of four siderostats with an aperture of 35 cm and a metrology plate placed in a hut and solidly anchored on bedrock and placed in an insulated chamber thermally stabilised to 0.1 °C. They constitutes three 20 m baselines and three 35 m baselines [11]. At the receiving end of the instrument, the light path and the control and recombining systems are common to all baselines.

In order to avoid a large number of instrumental parameters to be determined with Eq. (1), a sophisticated metrological system was constructed. The geometry of the ensemble is accurately measured using HeNe laser interferometers mounted in the huts and thermally stabilised to 0.1 °C. The goal is to monitor the motions of the pivot points of the siderostats, which determine the baselines during the course of the night with respect both to one another, and to local bedrock. This provides the components of the base vectors in a coordinate system fixed with respect to the bedrock. They are measured with a 100 nm precision [12]. Some remarkable points in this complex measuring ensemble are:

- the siderostat positioning consists of five interferometers pointed at the cat's eye reflector in the centre of the mirror. Its objective is to measure mirror motions with respect to a metrology plate with respect to which all geometric measurements are performed;
- each of the optical anchor systems consists of six HeNe interferometers situated at three corners of the metrology plate which measure the vertical motions of the metrology plate with respect to retroreflectors anchored on rock 7 metres below the soil surface;
- the pier to pier system connects the four metrology plates with eleven HeNe interferometers to monitor relative horizontal motions and rotations of the tables;
- the thermal expansion monitoring system is an interferometer that measures the thermal expansion of the metrology plate on which it is mounted.

Another important feature of the NPOI concerns the correction of refraction. The observations are performed in 32 spectral channels. The delay on each baseline is modulated by a small number of wavelengths, while, for each spectral channel and baseline, the photon count rates are synchronously measured, and a fringe visibility is obtained for each channel. This allows one to correct the atmospherically induced delay fluctuations that are averaged every 200 ms [12].

Tests of astrometric use of the NPOI have started only recently. Measurements of the siderostat pivot motion have shown a repetitiveness of 200 nm. The objective is to reach an accuracy of 1–3 mas for magnitudes up to 8 or 9 [11]. It can be also used for measuring star diameters. For instance, using the large non-astrometric baselines, the diameter of α Ari was measured with an uncertainty of 0.07 mas [8].

4.4. Very long baseline interferometry (VLBI)

If the application of optical stellar interferometry is still in a prototype stage, radio interferometry has been operational already for several decades. As in the case of optical interferometry, it was first designed as an imaging instrument in radiowaves. However, it was later used for astrometry, and we shall describe here only the astrometric applications.

The principle is the same that in the optical case. There exist several ensembles of interconnected radio telescopes. The largest is the Very Large Array (VLA) in New Mexico consisting of 27 identical 25 m dishes [13]. They can be moved on tracks in a Y shape configuration allowing baselines up to 35 km. Observing at $\lambda = 5$ cm, the best achievable resolution is 30 to 50 mas. Actually, combining several observations, such an angular accuracy on relative positions of radiosources was indeed obtained [14]. To obtain a better accuracy, one must increase the baseline. An approach is to provide the link between the receivers not by wires, but by a radio link. This is the case of the MERLIN array in Great Britain [15], which may include several radio telescopes with a maximum baseline of 217 km. It provides a resolution of about 40 mas at 5 MHz.

However, the actual solution is to register the received data on magnetic tapes and send them to a central computer, called correlator, which retrieves the fringes. The only limitation that remains is that the same object should be simultaneously visible from the two radio telescopes. This sets the limit to about 8000 km and justifies the name of the technique: Very Long Baseline Radio Interferometry, in short, VLBI.

An antenna transforms the electromagnetic field of a radio wave into an electric potential, V , proportional to the instantaneous amplitude of the wavefront

$$V = b \cos(\omega - \phi),$$

where ϕ is the phase of the wave to which a constant instrumental dephasing is added. A local oscillator, generally a hydrogen maser, produces a stable reference frequency and a current

$$V' = b' \cos \omega_0 t,$$

where ω_0 is close to ω .

These frequencies are mixed in a special heterodyne circuit. After filtering out high frequency terms, there remains a periodic electrical intensity proportional to bb' with an angular frequency $\omega - \omega_0$ and the same phase ϕ

$$I \sim bb' \cos[(\omega - \omega_0)t - \phi]. \quad (6)$$

Choosing ω_0 in such a way that the frequency of $\omega - \omega_0$ is of the order of 2 MHz, it is now possible to sample this frequency and represent numerically on a tape the time variations of (6). The timing is accurately marked on the same tape.

At a second radio telescope the same procedure is followed on the same radio source. Then both recordings are brought together and compared. The better the local clocks are synchronised, the better one can recognise that the two records correspond to the same wavefront. An approximate reckoning of the path difference produces a first approximation to the time delay is the start point of the correlation between the two signals. The correlator computes a normalised correlation function, which is maximum for the exact value of the delay.

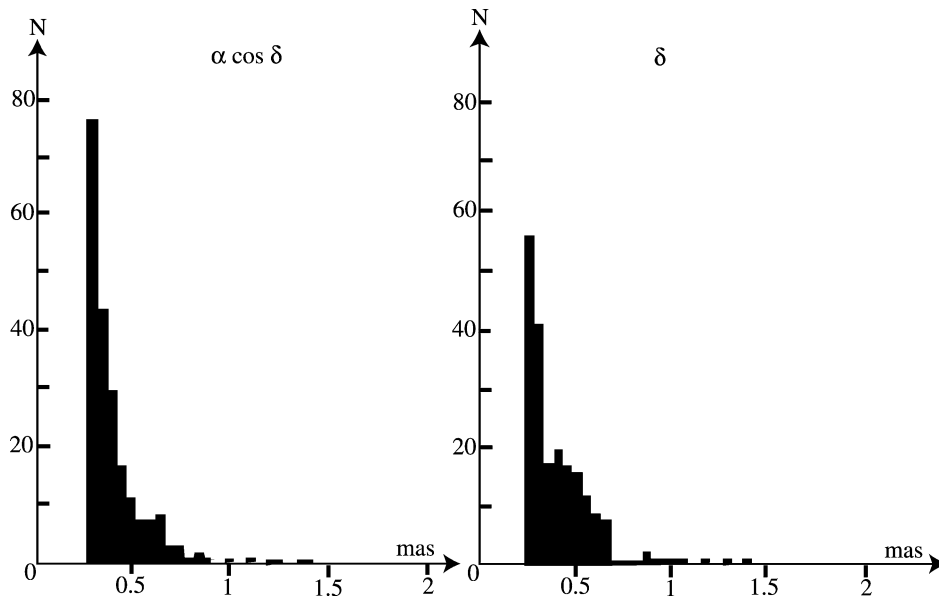


Fig. 2. Histograms of uncertainties in the coordinates of the 212 defining radio-sources of the International Celestial Reference frame, ICRF [16].

The actual determination of the time delay at a reference instant is a very complex procedure. One must first correct for the unknown ionospheric and tropospheric refractions. This is done by observing simultaneously at two frequencies, the S band (2300 MHz) and the X band (8400 MHz). One must also take into account the continuous variation of the received frequency due to the Doppler shift produced by the rotation of the Earth.

In order to increase the precision of the result one separates the observed band into 28 channels of 2 MHz bandwidth, and makes simultaneous correlations on a parallel computer.

The fundamental equation applied to interpret the data is formula (3). So VLBI can be used to determine the baseline, assuming the celestial coordinates of the sources, usually quasars, are known. This gives information both on the geodetic position of the antennae and the parameters of the rotation of the Earth. Conversely, knowing the position of antennae and the elements of Earth rotation, one can determine the directions, \mathbf{S} of sources.

Actually, there are too many parameters to be determined from a single baseline. So, networks of several radio telescopes are operated for any observing program. The uncertainty of a single observation of a source is about 5 mas, but synthetic treatment of many baselines gives the parameters of the rotation of the Earth with uncertainties of about 0.2 mas.

Similarly, the global treatment of many VLBI observations significantly decreases the uncertainty of source positions. As an example, an important program of determination of the positions of extragalactic radiosources using the results of several VLBI networks in order to set up a non-rotating celestial reference frame was performed. Fig. 2 gives the histogram of the uncertainties in right ascension ($\alpha \cos \delta$) and declination (δ) for the 212 sources retained to represent this frame [16].

Furthermore, the positions of about 20 radio telescopes contributing to the VLBI networks were determined with uncertainties of the order of 0.5 mm. They are the primary net of positions upon which the International Terrestrial Reference Frame (ITRF) is based and tectonic plate motions are described.

A basic book on VLBI is [17]. Its applications to astrometry are discussed in [18].

5. Space techniques

Ground-based optical astrometry has several fundamental limitations, which are due to the atmospheric and gravitational environment that cannot be avoided, unless making observations from outer space. The advantages of space astrometry are essentially the following:

- absence of atmospheric refraction so that the apparent direction does not change with the angle of view;
- absence of atmospheric turbulence so that the image is a diffraction limited pattern, which can be more accurately, defined and analysed than on the Earth;
- quasi-absence of mechanical torques that deforms the instrument and modify the position of the image in the focal surface;

- the entire sky is observable with a single instrument;
- a very good temperature control.

On the other hand, in addition to it being very expensive, there is no access in case of failure and the instrument is lifetime limited. However, the main problem of space astrometry is the instability of the orientation of a satellite. It may vary quickly and irregularly, while an Earth-based instrument, fixed to the ground, has a well monitored motion in space. This largely complicates the engineering and the observing procedures.

As a consequence, a space astrometry mission is acceptable to space agencies only if it brings a considerably larger number of results with greatly improved accuracies than what might be expected from a great ensemble of ground-based telescopes. This was the case of Hipparcos, a European Space Agency satellite decided in 1980 and launched in 1989. Now, there are other space astrometry programmes that are approved and will be also presented.

5.1. The Hipparcos satellite

Hipparcos is a global astrometry instrument. Although stars are observed one by one, they all contribute to a solution in which all the unknown angles are determined. It is conceived to measure, and in due course to determine, large and small angles on the sky. Both the second and the third method described in Section 2 are used. There is also a solid reference angle, but although the actual final reference is the circumference, it serves as an intermediate standard. However, its fundamental role is to prevent propagation of errors and large correlations between star positions that would be unavoidable had a single telescope scanned the sky. This will be commented upon in Section 5.3.

Light enters through two baffles and falls on a complex mirror or beam-combiner, which is a 29 cm mirror cut into two halves and glued. Thus, Hipparcos observes simultaneously two fields of view whose centres are separated by the reference (basic) angle. Its value is

$$\gamma = 58^{\circ}0'31.25''.$$

Rays from star fields converge into a single focal plane (Fig. 3). The images I_1 and I_2 of stars S_1 and S_2 in different fields of view are formed on a grid, which modulates them while the satellite rotates about an axis parallel to the intersection of the mirrors of the beam combiner.

The orientation of the satellite (we shall use the word ‘attitude’, in accordance with the space technique jargon) is monitored by a system of vertical and inclined slits called the ‘star-mapper’ and by gyroscopes.

In the focal surface, manufactured on a silicon substrate, are the grids. In the centre is the main grid consisting of 2688 slits whose period, as measured in projection on the sky, is $1.208''$ with 39% transparent width. This covers a field of 0.9° by 0.9° on the sky. On either side of the main grid are two star-mappers. They consist of four vertical slits, the width of which is $0.9''$ and the separation respectively $a, 3a, 2a$ with $a = 5.625''$, and of a second system of four similarly separated slits but inclined by 45° in a chevron configuration. The light modulated by the star-mapper grid is transmitted to a dichroic plate, which

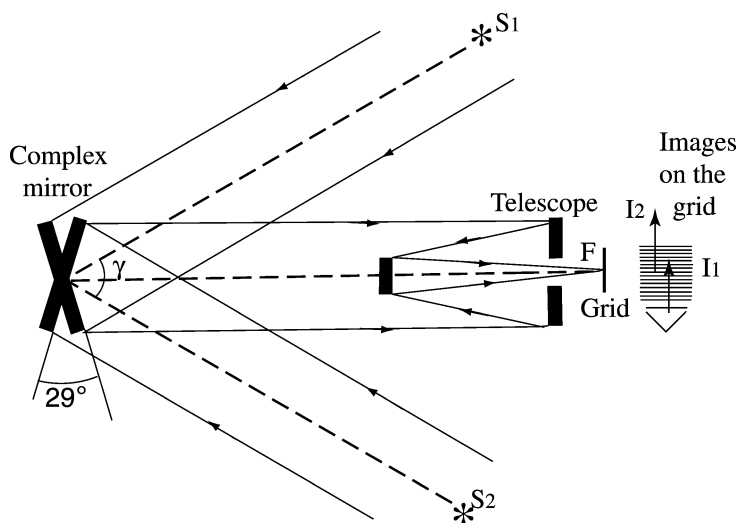


Fig. 3. Principle of Hipparcos.

splits the beam into two wavelength ranges. Photomultipliers sample the received light intensity with a frequency of 600 Hz. Star-mappers are used, together with gyroscopes, to monitor the orientation of the satellite.

While all stars present in one of the eight slits of the active star-mapper contribute to the signal, such a scheme was not suitable for the main grid because several stars are simultaneously present in the fields of view whereas each of the modulated star images must be registered independently. The separation is done electronically by an image dissector so that only a tiny part of the electronic image (30'' radius) enters into the receiver. The sampling of the incoming photoelectrons is performed at a frequency of 1200 Hz.

This approach implies that the positions of star images on the main grid are continuously known. This is possible only if one knows a priori the positions of the stars on the sky and that an accurate attitude is computed in real time on-board. This knowledge was provided by an Input Catalogue prepared in advance of the mission [19]. The primary determination of the attitude is obtained by the ESA satellite monitoring using the observations of star transits through the star-mapper and additional information from the gyroscopes.

A detailed description of the satellite and of the payload can be found in [20].

5.2. Hipparcos raw data reduction

In order to achieve the most regular coverage of the sky during the mission and in the same time to minimise straylight from the Sun, a nominal scanning law is imposed to the satellite rotation axis. The rotation period was 2 h 8 min and the axis of rotation processed around the direction of the Sun in 57 days. This ensured an overlap between two successive scans. Each time, the actual attitude deviated from the nominal scanning law by more than 10', gas jet actuators were activated so as to reverse the natural attitude trend. This generally happened about 12 times per satellite rotation.

Two photon count data streams were received by the two data reduction consortia. The star-mapper data and the main grid data.

The main grid data was divided into 2.133 s observation frames during which all stars present in the fields of view were sequentially observed by the image dissector. The photon counts for a given star were represented by a Fourier series limited to the second order:

$$I(t) = I_0 + B + I_0 M_1 \cos(\omega(t - t_0) + \phi_1) + I_0 M_2 \cos 2(\omega(t - t_0) + \phi_2). \quad (7)$$

Here, B is the sky background. The angular frequency ω is determined from the duration of the crossing of one grid step and ϕ is a phase that describes the position of the image with respect to the centre of the grid at the time origin. For a single star, $\phi_1 = \phi_2$. If they are not equal, this is an indication that the star is double or multiple. Translated into angles on the sky, the uncertainties of the phase determination in a single frame and, in the mean observed 0.5 s, are:

- 11 mas for a star of magnitude 8; and
- 17 mas for a star of magnitude 9 (2.5 times fainter).

The star-mapper photon counts for a given star are used to determine the time of transit through a conventional mean slit. Expressed in angles on the sky, the uncertainties are:

- for a star of magnitude 8, 25 mas (vertical slit) and 35 mas (inclined slit); and
- for a star of magnitude 9, 40 mas (vertical slit) and 55 mas (inclined slit).

5.3. Great circle reduction

The next step is to combine the data into larger ensembles. The natural choice was to take all the observations during a satellite orbit, that is 7 to 9 consecutive hours. During this time, the scanning varies by a few degrees, and only the along-scan measurements are significant (with the exception of the inclined slits of the star-mapper). So, all the observations were projected on a single conventional mean great circle with a conventional origin, Ω , called 'Reference Great Circle' (RGC).

We shall not describe the reduction procedure, which includes many calibrations and coordinate transformations. A detailed description of all the phases of the computation can be found in [21, vol. 3]. Let us make only a remark on attitude determination. Indeed, a major task is to retrieve the attitude and to represent it by some analytical expressions. The theory is described in [22]. Here, the Euler angles of attitude are represented for the duration of one rotation of the satellite by Fourier series to which impulsive functions are added at each gas jet actuation. This is sufficient for two angles. But the along-RGC component, which must be represented with the same accuracy as the final star positions, the number of parameters to be determined becomes excessive. The solution retained was to represent it by a series of cubic splines.

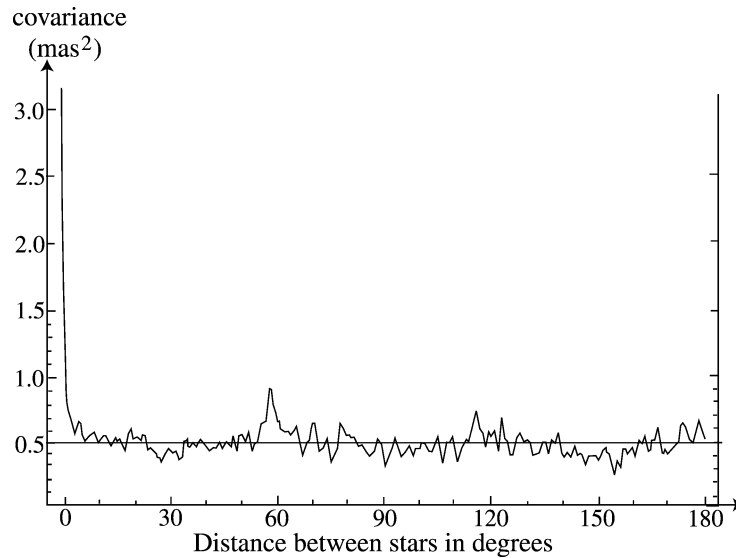


Fig. 4. Averaged auto-covariance function of the star abscissa.

The grid coordinates of a star image are projected on the sky and then on the RGC, so that one gets of the order of 40–50 thousand observed star coordinates. These are functions of the actual coordinates of the star, the orientation at the time of observation, the grid-to-sky transformation, and the basic angle. Approximate values of the parameters are available and permit linearising the equations. The unknowns are:

- abscissae on the RGC of 1000–1300 stars;
- about 1000 cubic spline coefficients representing the attitude along the RGC;
- 40 grid-to sky transformation parameters;
- a correction to the value of the basic angle.

It is possible to determine the latter, because the standard used is the circumference, materialised by stars, which do not move between two transits separated by one rotation of the satellite. The uncertainty obtained for the basic angle is 0.3 mas.

It should be pointed out that positions of stars observed simultaneously are strongly correlated. If there were a single field of view, the correlation would propagate along the great circle. The fact that they are observed simultaneously with stars at $\pm\gamma$ dilutes considerably this correlation, as shown in Fig. 4. The value of γ was optimised so as to minimise this effect, which is still apparent at γ and 2γ from the origin [23]. In particular, choosing a basic angle that would be too small, or be a rational fraction of the circumference, would have greatly increased this undesirable effect. Actually, because of the scanning law, the regions of the sky which are observed simultaneously, vary at random and this effect disappears in the global solution described in the next section.

The mean uncertainty of the determination of the abscissa on an RGC of bright stars (magnitude less than 10), was 3 mas.

5.4. Determination of astrometric parameters

During almost three years of operation of the mission, about 2000 RGC solutions were obtained. Each of the 118 000 stars in the programme was observed 25 to 50 times. The problem was to link them and to determine their positions in a single reference system. To define this, the conventional origins of the RGCs were shifted by a quantity $\Delta\Omega$ in such a way that there is consistency between the relative positions of all the stars.

While one could ignore the displacements of stars during a few hours, it is no longer possible for longer times. They must be modelled. Five parameters, called astrometric parameters, are necessary:

- the two coordinates (right ascension α_0 and declination δ_0 of the star at some defined epoch, actually, 1991.25);
- the annual proper motion in each of these coordinates, μ_α and μ_δ ;
- the annual parallax, which is the semi-major axis of an ellipse inversely proportional to the distance of the star.

The abscissa of a star S on the RGC is the angle, along the RGC, between the projection of the position of star at the time of observation and the origin of the RGC corrected by $\Delta\Omega$. The value obtained at the RGC reduction is equated to it. With the 40 000 best observed stars, one gets a system of 1 200 000 equations with 202 000 unknowns.

Eliminating the astrometric parameters of stars, one is left with a system of equations, which is solved for the origin shifts. The result is incorporated in the equations relative to each star. The solution gives the five astrometric parameters.

5.5. Iterations and results

This is not the final result. The coordinates that are obtained are polluted by the approximations in the a priori star positions that are good only to a fraction of an arcsecond. These uncertainties affect essentially the attitude determination and the reduction on a RGC. So, the whole procedure, except the raw data treatment, is repeated with the newly obtained astrometric parameters, until the results converge. The final results for 117 955 stars are:

- median uncertainty in positions at 1991.25, in α_0 , 0.77 mas, in δ_0 , 0.64 mas;
- median uncertainty in yearly proper motions, in α , 0.88 mas/yr, in δ , 0.74 mas/yr;
- median uncertainty in parallaxes, 0.97 mas.

In conclusion, space astrometry with Hipparcos has globally an uncertainty better than one milliarcsecond.

5.6. TYCHO

Once the final attitude is determined, the data collected by the star-mapper can be used, as observations of star positions. Since all stars in the field of view are registered, position parameters could be obtained for more than 2 500 000 stars. A first catalogue, called the TYCHO Catalogue, includes the 1 058 332 best observed stars up to visual magnitude 10.5. It has a median uncertainty in star position of 7 mas. The reduction procedure is fully described in [21, vol. 4]. No attempt was made to estimate the other astrometric parameters.

Later, the TYCHO 2 Catalogue was constructed; it includes 2 538 913 stars [24]. The stellar positions at epoch close to 1991.25 for the additional stars do not have such good uncertainties. These range between 7 and 90 mas.

5.7. HST astrometric capabilities

Although it was not a major objective, the Hubble Space Telescope is able to perform some small field astrometric observations. There are two astrometric modes.

1. Two Fine Guidance Sensors (FGS) are used for guiding the telescope on stars. A third one is available for measuring relative positions of stars in a 90° annulus within $11'$ and $14'$ from the centre of the field. The description of the design, modes of operation, and calibration are given in [25]. The precision is of the order of 3.5 mas for a series of observations lasting between 10 and 20 minutes.
2. The Wide Field and Planetary cameras equipped with CCDs, have respectively $2.7' \times 2.7'$ and $1.2' \times 1.2'$ fields of view. They can register objects up to magnitude 28. The relative positions of objects can be recovered as described in Section 2.3 using the pre-calibrated properties of the receiver. However, the star images are undersampled, leading to a complex observing and reduction procedure [26]. This mode is rarely used and only on specific cases of very faint objects. The uncertainty of determining relative positions is 2 mas up to magnitude 25, degrading to 10 mas for magnitude 28.

6. Future space missions

Two astrometric space missions are approved and the payloads are in a well advanced stage of detailed definition, with prototypes of the most critical elements being built.

6.1. Space interferometry mission (SIM)

Ground-based interferometry is very dependent on a perfect knowledge of the atmospheric refraction and too sensitive to local turbulence. The idea is to adapt interferometric techniques to space. Although, even on ground, visual astrometric interferometry is most difficult, so that the existing instruments are still considered as being prototypes, NASA has programmed

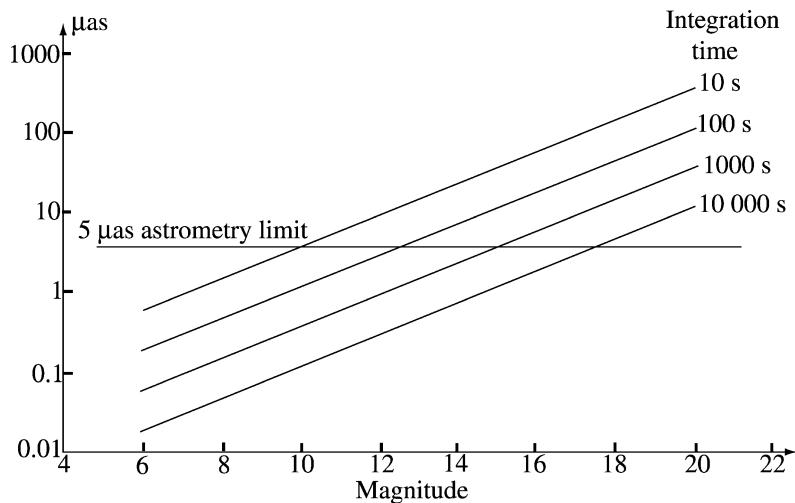


Fig. 5. Photon limited uncertainties of SIM observations as functions of magnitude and integration times.

for 2009–2010 a space interferometer, SIM, with astrometric objectives. This is because, even with a small base, the expected gain is considerable.

The US Space Interferometry Mission (SIM) is an orbiting stellar interferometer consisting of two siderostats with equal apertures of 30 cm collecting the light with a distance of 7 meters. In addition, each pod has two steerable mirrors which are the collectors of two guide interferometers directed towards bright stars and are used to determine the orientation in space of the baseline during the observation period. The collected light is directed towards delay lines and a beam combiner. An accurate positioning of the collecting mirrors with respect to the beam combiner will be performed by infrared stabilised interferometers with an absolute accuracy of 1 μm per meter. During its five years of operation, about 10 000 objects as faint as magnitude 20 should be observed. The expected uncertainty depends on the number of photons received that is on the observation time and on the magnitude of the object. This is illustrated by Fig. 5. For narrow angle ($< 1^\circ$) astrometry, one expects to reduce uncertainties to 0.5 μas .

The main objectives of SIM are the search of planets around near-by and young stars, the motions and distances of near-by galaxies, the motions and deformations of nuclei in galaxies, the masses of dark objects by micro-lensing and the motion of the Galaxy in an extragalactic reference frame.

6.2. GAIA (Global Astrometry Instrument for Astrophysics)

GAIA is a programmed ESA satellite to be launched in 2010–2011. Following the success of Hipparcos, it is based upon the Hipparcos main principles with two fields of view separated by 106° [27]. It is intended to be placed on an orbit around the Lagrange point L2 of the Earth–Sun system. This point is an equilibrium point in the Sun–Earth–GAIA configuration. It allows a cheap orbital control in terms of energy, and leaves in the same region of the sky the main disturbing light sources, which are the Sun, the Earth, and the Moon so that they are easy to avoid by an adequate scanning law. The astrometric instrumentation consists of two telescopes with a rectangular entrance pupil whose dimensions are 140×50 cm with a 46.7 m equivalent focal length.

The common focal plane covers a field of view of $0.66^\circ \times 0.66^\circ$. It is filled with some 170 CCDs operating in drift scanning mode. In this mode, the charge transfer of the CCD rows has exactly the speed of rotation of the satellite (full rotation in 6 hours), so that the photons of a given object always accumulate on the same drifting image, allowing an exposure of 40 seconds.

Each CCD has 2780 pixels along track by 2150 pixels in the perpendicular direction. Along track, this represents on the sky an angle of 43 mas.

The first two columns of the mosaic are star-mappers, which detect images above some given threshold and determine their positions and speeds in the focal plane. Then the image reaches the astrometric CCDs and the five broad bands photometers. Only small pixel windows around the predicted path are read and transmitted to the ground after some on-board treatment.

The expected accuracies of positions and parallaxes for a 5 year mission, range from 4 μas for stars up to magnitude 12, to 160 μas for magnitude 20. The accuracy of yearly proper motions should be of the same order of magnitude, but, as in the case of Hipparcos, it depends upon the latitude of the object. Fig. 6 gives the expected accuracy curves as functions of magnitude and ecliptic latitude.

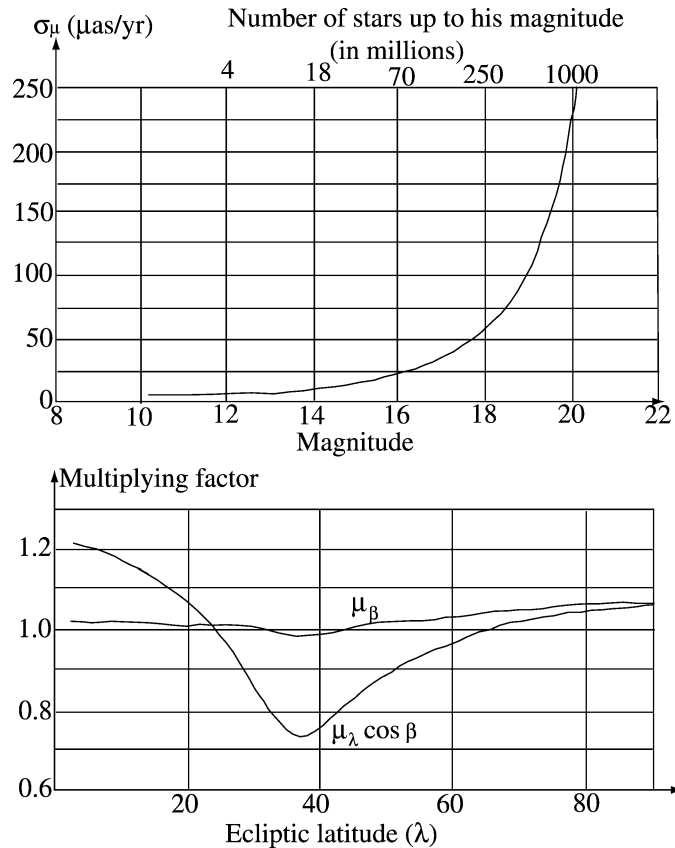


Fig. 6. The upper graph shows the expected accuracy of the positions obtained by GAIA after a 5 year mission as a function of the magnitude. The upper line gives the expected number of objects up to that magnitude. The lower graph gives the factor by which the accuracies of the upper graph must be multiplied to get the uncertainty in proper motions in ecliptic latitude (μ_β) and longitude ($\mu_\alpha \cos \beta$).

A third telescope allows GAIA to provide two additional parameters that are very important for the astrophysical interpretation of the astrometric data. The first is the radial velocity of all stars up to magnitude 16–17 with an accuracy ranging from 1 to 10 km/s. This is obtained by analysing the spectrum around the CaII triplet in the 845–875 nm bandwidth. Radial velocity is a component of the space velocity of objects whose determinations were scarcely distributed and could not be consistently used in galactic dynamics. The second instrument is a medium-band photometer recording in 10 different spectral bands, providing a good estimation of the spectral class of all the stars up to magnitude 20.

The scientific objectives of GAIA are extremely wide and diversified. Some examples are given below.

- In our Galaxy, analysis of the spatial and dynamic structure of the Galaxy, its bar and halo, the kinematics of various stellar populations leading to its formation and evolution history, mass function and luminosity function in the solar neighbourhood, large sky survey for extra-solar planets (20 000?).
- Beyond our Galaxy, distance standards for the local group, quasar detection, redshifts, microlensing structure, non-rotating reference frame to a few tenths of a μas per year.
- In stellar astrophysics, a rigorous framework for stellar structure and evolution theories, comprehensive luminosity calibration, initial mass and luminosity function in star forming regions, detection and characterisation of all spectral types and variable stars.
- In the Solar system, large scale survey of Solar system bodies (100 000?).
- The post-Newtonian parameter γ to 10^{-7} accuracy.
- Etc.

This includes most of the objectives of SIM at a much larger scale, with the exception of programmes that need high astrometric accuracy for faint objects.

7. Expectations for the more remote future

The remarkable jump in accuracy and in number of objects from Hipparcos to GAIA is due essentially to three factors: multiplying by 25 the collecting surface, by a factor of 10 to 15 the efficiency of the detector, and the fact that all objects present in the fields of view are observed during all the transit of the field of view. Additional improvements may be possible, but they seem to be marginal. The only parameter for which it is desirable to increase considerably the accuracy is the radial velocity. It is to be expected that future efforts will be directed towards higher resolution spectra and finer modelling and retrieval of the centre of spectral lines. The associated astrometry should however be improved by a factor of 10, because GAIA does not survey with a sufficient precision the central parts of the Galaxy.

On the other hand, SIM is a very small interferometer. Larger baselines are quite possible within a factor ten or so for a solid base interferometer. However, if one has a constellation of independent receivers, each on a different space vehicle, and the observations are transmitted to a central correlator, there is no limit in the dimension of the net. Of course, it will be necessary to have a very accurate relative positioning of the receivers by laser interferometry. This would be the extension to space and optical wavelengths of the VLBI principle, and it is already advocated by Antoine Labeyrie [28]. If this is realised, the accuracy of the astrometric measurements may be as good as a nanoarcsecond.

References

- [1] P. Benevides-Soares, R. Boczko, *Astron. Astrophys.* 96 (1981) 127–132.
- [2] H. Eichhorn, *Astronomy of Star Positions*, Ungar, New York, 1974.
- [3] J. Kovalevsky, *Modern Astrometry*, Springer-Verlag, Heidelberg, 2002.
- [4] M. Shao, M.M. Colavita, B.E. Hines, et al., *Astron. Astrophys.* 193 (1988) 357–371.
- [5] M. Shao, M.M. Colavita, Long-baseline optical and infrared stellar interferometry, *Annu. Rev. Astron. Astrophys.* 30 (1992) 457–498.
- [6] R. Hanbury Brown, *The Intensity Interferometer*, Taylor and Francis, London, 1974.
- [7] J.A. Benson, D.H. Hutter, N.M. Elias, et al., *Astron. J.* 114 (1997) 1221–1226.
- [8] A.R. Hajian, J.T. Armstrong, C.A. Hummel, et al., *Astrophys. J.* 496 (1998) 484–489.
- [9] X.P. Pan, M. Shao, M.M. Colavita, et al., *Astrophys. J.* 384 (1992) 624–633.
- [10] C.A. Hummel, D. Mozurkewich, J.T. Armstrong, et al., *Astron. J.* 116 (1998) 2536–2548.
- [11] J.T. Armstrong, D. Mazurkewich, L.J. Richard, et al., *Astrophys. J.* 496 (1998) 550–571.
- [12] D.J. Hutter, in: K.J. Johnston, et al. (Eds.), *Towards Models and Constants for sub-milliarcsecond Astrometry*, IAU Colloquium 200, US Naval Observatory, Washington, DC, 2000, pp. 47–56.
- [13] A.R. Thompson, B.G. Clark, C.M. Wade, P.J. Napier, *Astrophys. J. Suppl.* 44 (1980) 151–167.
- [14] D.R. Florkowski, K.J. Johnston, C.M. Wade, C. De Veigt, *Astron. J.* 90 (1985) 2381–2386.
- [15] Thomasson, Q. J. Roy, *Astron. Soc.* 27 (1986) 413–431.
- [16] C. Ma, E.F. Arias, T.M. Eubanks, et al., *Astron. J.* 116 (1998) 516–546.
- [17] M. Felli, R.E. Spencer, *Very Long Baseline Interferometry, Techniques and Applications*, Kluwer Academic, Dordrecht, Netherlands, 1989.
- [18] H.G. Walter, O.J. Sovers, *Astrometry of Fundamental Catalogues*, Springer-Verlag, Berlin, 2000.
- [19] M.A.C. Perryman, C. Turon (Eds.), *The Hipparcos Mission, Pre-Launch Status, vol. 2, The Input Catalogue*, ESA SP 1111, European Space Agency, Paris, 1989.
- [20] M.A.C. Perryman, H. Hassan (Eds.), *The Hipparcos Mission, Pre-Launch Status, vol. 1, The Hipparcos Mission*, ESA SP 1111, European Space Agency, Paris, 1989.
- [21] ESA, *The Hipparcos and Tycho Catalogues*, ESA Publication SP-1200, 17 volumes, Paris, 1997.
- [22] J. Kovalevsky, E. Bois, in: K.B. Bhatnagar (Ed.), *Space Dynamics and Celestial Mechanics*, Reidel, Dordrecht, Netherlands, 1986, pp. 345–354.
- [23] H. Van der Marel, C. Petersen, *Astron. Astrophys.* 258 (1992) 60–69.
- [24] E. Høg, C. Fabricius, C.C. Makarov, et al., *Astron. Astrophys.* 357 (2000) 367–386.
- [25] R.A. Ibata, G.F. Lewis, *Astron. J.* 116 (1998) 2569–2573.
- [26] R.L. Duncombe, W.H. Jefferys, P.J. Shelus, *Adv. Space Research* 11 (2) (1991) 87–96.
- [27] ESA, *GAIA, Composition, Formation and Evolution of the Galaxy; Concept and Technology Study Report*, ESA Publication ESA-SCI(2000), 4, 2000.
- [28] A. Labeyrie, personal communication.